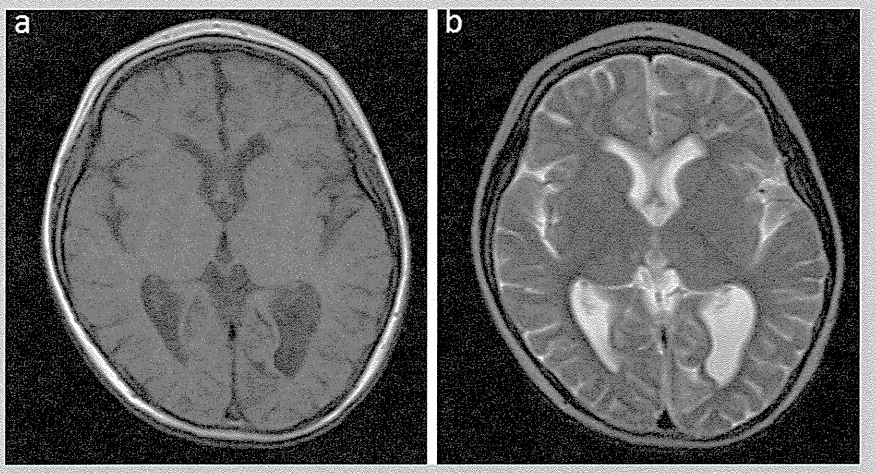

FIG. 1. a,b: Brain magnetic resonance imaging (MRI) of the patient at 4 years of age. T1-weighted (a) and T2-weighted (b) axial images of the patient showed diffuse cortical atrophy, enlarged lateral ventricles, and delayed myelination. Abnormal findings in the globus pallidus and substantia nigra were not detected.

by normal delivery. Her birth parameters included weight 2,930 g, length 47 cm, and occipitofrontal circumference 30 cm. Developmental delay was not noticed before 10 months of age. She was able to sit without support at 14 months of age. She showed stereotyped behavior, including hand wringing and finger sucking. Eye contact was poor. She was initially diagnosed with Rett syndrome (RTT). She suddenly lost consciousness and dropped her head slowly. She was diagnosed with epilepsy, and she was treated with valproic acid. Her EEG showed diffuse spike-wave and polyspike-wave bursts. Brain MRI study at 4 years of age with routine T1-weighted and T2-weighted imaging showed delayed myelination and enlarged lateral ventricles. No signal abnormalities indicating iron accumulation existed (Fig. 1a,b).

At 5 years of age, physical examination identified a series of dysmorphic features, including hypertelorism, epicanthal folds, flat nasal bridge, bilateral low-set ears, downslanting palpebral fissures, short philtrum, high palate, downturned mouth and micrognathia (Fig. 2). Hearing was normal. She showed spasticity of the lower extremities. She was unable to walk independently. Her mental development was significantly delayes. She had no communicative language. She could reach objects and shift toys between hands. Behavioral abnormalities, including bruxism, finger sucking, temper outbursts were observed. Her height was 111 cm (0.3 SD), weight was 19.5 cm (0.4 SD) and head circumference was 49 cm (−0.9 SD).

She showed constantly increased serum enzymes. The level of aspartate transaminase (AST, 62–106 U/L; nl <32 was higher than that of alanine transaminase (ALT, 13–20 U/L; nl <31). Serum creatine kinase (CK), aldolase and neuron specific enolase (NSE) were also mildly elevated. Investigations for metabolic disorders and routine cytogenetic studies were normal. Molecular studies for RTT and array-comparative genomic hybridization (array-CGH) analysis gave normal results. We therefore planned a proband-parent trio approach using whole exome sequencing. As a result, she was diagnosed with BPAN.

At 6 years of age, T2*-weighted MR imaging and T2 star-weighted angiography (SWAN) demonstrated hypointense signals in the GP and SN (Fig. 3a–d). We assume that these signals indicate iron accumulation. Routine T1-weighted and T2-weighted imaging showed only cerebral atrophy.

FIG. 2. Face of the patient at 5 years of age (with permission).

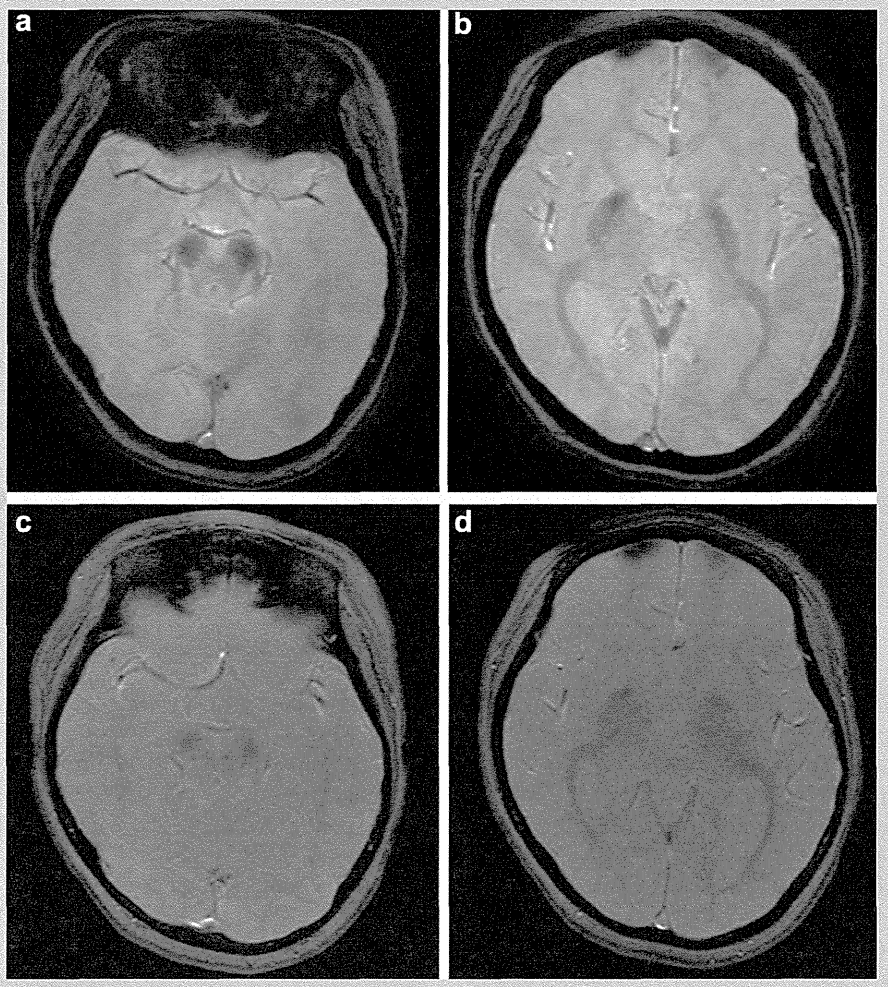

FIG. 3. MRI of the patient at 6 years of age. T2*-weighted (a,b) and SWAN (c,d) axial images of the patient at 6 years of age showed hypointensity in the substantia nigra and the globus pallidus, consistent with iron accumulation.

MATERIALS AND METHODS

Exome and Sanger Sequencing

Informed consent was obtained from the parents, in accordance with the Declaration of Helsinki, and the study was approved by the ethics committee of Osaka Medical Center and Research Institute for Maternal and Child Health (Osaka, Japan) and The University of Tokushima (Tokushima, Japan).

Genomic DNA was obtained from peripheral-blood leukocytes by standard methods, captured with the TrueSeq™ Exome Enrichment Kit (Illumina, San Diego, CA), and sequenced with three samples per lane on a HiSeq 1000 platform (Illumina) with the 101-bp paired-end reads. Image analysis and base calling were performed with sequence control software real-time analysis and CASAVA software v1.8 (Illumina) with default parameters. Reads were aligned to the human genome assembly hg19 (GRCh37) as a reference with the Burrows-Wheeler Alignment tool (BWA) 0.6.1. (http://bio-bwa.sourceforge.net/). Duplicate reads were marked using Picard 1.7.5 (http://picard.sourceforge.net/) and excluded from downstream analysis. Local realignments around indels and base quality score recalibration were performed with the Genome Analysis Toolkit (GATK) 1.6 (http://www.broadinstitute.org/gatk/). Single-nucleotide variants and small indels were identified using the GATK UnifiedGenotyper and filtered according to the Broad Institute's best-practice guidelines. Variants that passed the filters were annotated using snpEff V3 (http://snpeff.sourceforge.net/index.html) and ANNOVAR (http://www.openbioinformatics.org/annovar/). After merging the VCF files of all members of the family, we filtered variants to exclude those present in dbSNP132 (http://www.ncbi.nlm.nih.gov/projects/SNP/) and the 1000 genomes project database (http://www.1000genomes.org/) with average heterozygosity $\geq$0.01. Summary of the exome sequencing performance is as shown in Supplementary Table SI (see Supporting Information online). Sanger sequencing confirmed each variant identified.

X-Inactivation Analysis

The X-inactivation pattern was studied using the human androgen receptor (HUMARA) assay [Kubota et al., 1999]. Briefly, genomic DNA from the subject and control females was digested with two methylation-sensitive enzymes, HpaII and HhaI. PCR was performed using a primer pair of FAM-labeled HUMARA 1F: CCAGAATC TGTTCCAGAGCGTGC and HUMARA 1R: CTCTACGATGGG CTTGGGGAGAAC. Fluorescently labeled products were analyzed on an ABI PRISM 3500 Genetic Analyzer with GeneMapper Software version 4.0 (Life Technologies, Carlsbad, CA).

RESULTS

All the novel nonsynonymous and frameshift variant calls were subjected to direct nucleotide sequence analysis using Sanger sequencing for confirmation. Candidate variants corresponding to de novo events or an autosomal recessive model, including compound heterozygosity are shown in Supplementary Table SII (see Supporting Information online). We evaluated the pathogenic significance of each variant. Among the candidate variants, she had an early termination codon in exon 11 of the *WDR45* gene due to a non-sense mutation (c.C868T:p.Q290X). We confirmed this mutation in *WDR45* by direct nucleotide sequence analysis using a primer pair of WDR45 1F: TCTCAAGGATACCCGCCTC and WDR45 1R: ATGACAGAGTTGACGTTCTTG (Supplementary Fig. S1—see Supporting Information online). This mutation was not observed in her parents or in the central resource recently provided to archive and display Japanese genetic variation determined by exome sequencing of 1,208 Japanese individuals (Human Genetic Variation Browser from Japanese genetic variation consortium, http://www.genome.med.kyoto-u.ac.jp/SnpDB). Since mutations causing early termination around the mutated site in this patient were frequently observed in other cases of BPAN (1–3), the observed mutation of *WDR45* (c.C868T:p.Q290X) seems to cause BPAN in this patient.

As shown by Saitsu et al. [2013], X-inactivation analysis with genomic DNA from peripheral leukocytes showed a marked skewing pattern (96:4) in the patients compared with her mother (50:50). However, it is unknown whether the wild-type allele underwent X inactivation in the leukocytes as well as brain tissues of the patient.

DISCUSSION

Using whole exome sequencing, we have identified a de novo nonsense mutation in the *WDR45* gene, which is likely to cause BPAN, in the 6-year-old Japanese girl with a series of dysmorphic features, severe developmental delay, and epilepsy. She showed RTT-like features. Characteristic MRI findings of BPAN were evident at 6 years of age. Since there are no reports of the dysmorphic features of BPAN, it is unclear whether these features are common to other patients. Further detailed analysis of BPAN cases will be needed, although it is possible that other genetic variations/alterations observed in this patient may modify phenotypes of BPAN.

Patients with BPAN are reported to begin walking at 2–3 years of age [Haack et al., 2012; Hayflick et al., 2013; Saitsu et al., 2013]. Most patients are described as a clumsy child with a broad-based or ataxic gait. Some patients show spasticity. Our patient could not walk alone, but could stand with support at 6 years of age. The motor disability in our patient seems to be more severe than in the reported patients. Severe delay in language development is a constant feature in BPAN. Our patient had no communicative language and poor eye contact. Subjects reported by Saitsu et al. [2013] showed some stereotype movements such as hand wringing or flapping. Seven female patients of 23 BPAN cases reported by Hayflick et al. [2013] were suspected to have the atypical RTT, two of whom had repetitive midline hand-wringing behavior. Our patient also had been initially diagnosed with RTT, although preserved hand movement, dysmorphic features and spasticity were distinct from typical RTT patients. Verhoeven et al. [2014] showed that neuropsychiatric symptoms within the autistic and affective spectrum were present in the early phase of the disease. They reported that progressive cognitive and motor deterioration with dystonia and Parkinson symptoms emerge in the course of BPAN.

Through examination of autopsied RTT brains, hypofunction of the nigrostriatal dopamine neurons is proposed to be involved in modulating posture and locomotion [Segawa, 2005]. In addition, dystonia and Parkinsonism are commonly seen in older RTT patients [FitzGerald et al., 1990] and BPAN, indicating that SN dysfunction is involved in both RTT and BPAN. Although several features, for example, progressive microcephaly, have never been reported in BPAN, it is recommended that BPAN is considered in the patients with atypical RTT for differential diagnosis, and *WDR45* is analyzed before ages having typical brain MRI findings [Hayflick et al., 2013].

Serum AST, CPK, aldolase and NSE were mildly elevated. Abnormalities in laboratory data were not described in previous reports. Although the pathophysiologic mechanisms of elevated serum enzymes and their significance in the pathogenesis of BPAN remain unclear, it is possible that defects in the normal autophagic process caused by mutated WDR45 were associated with the elevation of serum enzymes through functional abnormalities in targeted tissues/organs.

Ohba et al. [2014] reported sequential brain MRI in a patient with BPAN. They reported that iron deposition in the GP and the SN was observed as early as 11 years of age. No aggravation of the neurological status was seen at that time. In our patient, T1-weighted and T2-weighted imaging showed only delayed myelination and an enlarged lateral ventricle. Iron accumulation in the GP and SN was not evident by these routine imaging. However, T2*-weighted MR imaging and SWAN revealed ion accumulation in the GP and SN at 6 years of age, indicating iron accumulation to be already present as early as this age. We suppose that high sensitive imaging methods including T2*-weighted MR imaging and SWAN are suitable for early detection of iron in BPAN patients.

In conclusion, we reported on a BPAN patient with a novel *WDR45* mutation before the onset of neuronal degeneration. Clinical manifestations in the first decade may mimic RTT, although the specific facial features and lack of microcephaly are distinct from *MECP2*-positive RTT patients. Elevation of serum AST, aldolase, CPK and NSE may result from abnormal autophagy. T2*-weighted MR imaging and SWAN may allow early detection of iron accumulation in the GP and SN as early as 6 years of age. These findings will be clues to diagnose BPAN before the appearance of

stereotypic features. Further studies are necessary to demonstrate early manifestations of BPAN.

ACKNOWLEDGMENTS

We thank for the family for their cooperation and the Support Center for Advanced Medical Sciences, Institute of Health Biosciences and Institute for Genome Research, the University of Tokushima Graduate School for technical assistance. This study was supported by the Health and Labour Research Grants in 2013 from the Ministry of Health, Labour and Welfare, Japan.

REFERENCES

FitzGerald PM, Jankovic J, Glaze DG, Schultz R, Percy AK. 1990. Extrapyramidal involvement in Rett's syndrome. Neurology 40:293–295.

Haack TB, Hogarth P, Kruer MC, Gregory A, Wieland T, Schwarzmayr T, Graf E, Sanford L, Meyer E, Kara E, Cuno SM, Harik SI, Dandu VH, Nardocci N, Zorzi G, Dunaway T, Tarnopolsky M, Skinner S, Frucht S, Hanspal E, Schrander-Stumpel C, Héron D, Mignot C, Garavaglia B, Bhatia K, Hardy J, Strom TM, Boddaert N, Houlden HH, Kurian MA, Meitinger T, Prokisch H, Hayflick SJ. 2012. Exome sequencing reveals de novo WDR45 mutations causing a phenotypically distinct, X-linked dominant form of NBIA. Am J Hum Genet 91:1144–1149.

Hayflick SJ, Kruer MC, Gregory A, Haack TB, Kurian MA, Houlden HH, Anderson J, Boddaert N, Sanford L, Harik SI, Dandu VH, Nardocci N, Zorzi G, Dunaway T, Tarnopolsky M, Skinner S, Holden KR, Frucht S, Hanspal E, Schrander-Stumpel C, Mignot C, Héron D, Saunders DE, Kaminska M, Lin JP, Lascelles K, Cuno SM, Meyer E, Garavaglia B, Bhatia K, de Silva R, Crisp S, Lunt P, Carey M, Hardy J, Meitinger T, Prokisch H, Hogarth P. 2013. Beta-propeller protein-associated neurodegeneration: A new X-linked dominant disorder with brain iron accumulation. Brain 136:1708–1717.

Kubota T, Nonoyama S, Masuno M, Imaizumi K, Kojima M, Wakui K, Shimadzu M, Fukushima Y. 1999. A new assay for the analysis of X-chromosome inactivation based on methylation-specific PCR. Hum Genet 104:49–55.

Ohba C, Nabatame S, Iijima Y, Nishiyama K, Tsurusaki Y, Nakashima M, Miyake N, Tanaka F, Ozono K, Saitsu H, Matsumoto N. 2014. De novo WDR45 mutation in a patient showing clinically Rett syndrome with childhood iron deposition in brain. J Hum Genet 59:292–295.

Saitsu H, Nishimura T, Muramatsu K, Kodera H, Kumada S, Sugai K, Kasai-Yoshida E, Sawaura N, Nishida H, Hoshino A, Ryujin F, Yoshioka S, Nishiyama K, Kondo Y, Tsurusaki Y, Nakashima M, Miyake N, Arakawa H, Kato M, Mizushima N, Matsumoto N. 2013. De novo mutations in the autophagy gene WDR45 cause static encephalopathy of childhood with neurodegeneration in adulthood. Nat Genet 45: 445–449.

Segawa M. 2005. Early motor disturbances in Rett syndrome and its pathophysiological importance. Brain Dev 27:S54–S58.

Verhoeven WM, Egger JI, Koolen DA, Yntema H, Olgiati S, Breedveld GJ, Bonifati V, van de Warrenburg BP. 2014. Beta-propeller protein-associated neurodegeneration (BPAN), a rare form of NBIA: Novel mutations and neuropsychiatric phenotype in three adult patients. Parkinsonism Relat Disord 20:332–336.

SUPPORTING INFORMATION

Additional supporting information may be found in the online version of this article at the publisher's web-site.

CLINICAL GENETICS An International Journal of Genetics, Molecular and Personalized Medicine

Clin Genet 2014

Published by John Wiley & Sons Ltd
CLINICAL GENETICS
doi: 10.1111/cge.12492

Short Report

Targeted next-generation sequencing in the diagnosis of neurodevelopmental disorders

Okamoto N., Miya F., Tsunoda T., Kato M., Saitoh S., Yamasaki M., Shimizu A., Torii C., Kanemura Y., Kosaki K.. Targeted next-generation sequencing in the diagnosis of neurodevelopmental disorders.
Clin Genet 2014. © John Wiley & Sons A/S. Published by John Wiley & Sons Ltd, 2014

We developed a next-generation sequencing (NGS) based mutation screening strategy for neurodevelopmental diseases. Using this system, we screened 284 genes in 40 patients. Several novel mutations were discovered. Patient 1 had a novel mutation in *ACTB*. Her dysmorphic feature was mild for Baraitser-Winter syndrome. Patient 2 had a truncating mutation of *DYRK1A*. She lacked microcephaly, which was previously assumed to be a constant feature of *DYRK1A* loss of function. Patient 3 had a novel mutation in *GABRD* gene. She showed Rett syndrome like features. Patient 4 was diagnosed with Noonan syndrome with *PTPN11* mutation. He showed complete agenesis of corpus callosum. We have discussed these novel findings.

Conflict of interest

The authors report no conflicts of interest.

N. Okamoto[a], F. Miya[b], T. Tsunoda[b], M. Kato[c], S. Saitoh[d], M. Yamasaki[e], A. Shimizu[f], C. Torii[g], Y. Kanemura[h,i] and K. Kosaki[g]

[a]Department of Medical Genetics, Osaka Medical Center and Research Institute for Maternal and Child Health, Osaka, Japan, [b]Laboratory for Medical Science Mathematics, Center for Integrative Medical Sciences, RIKEN, Yokohama, Japan, [c]Department of Pediatrics, Yamagata University Faculty of Medicine, Yamagata, Japan, [d]Department of Pediatrics and Neonatology, Nagoya City University Graduate School of Medical Sciences, Nagoya, Japan, [e]Department of Pediatric Neurosurgery, Takatsuki General Hospital, Osaka, Japan, [f]Division of Biomedical Information Analysis, Iwate Tohoku Medical Megabank Organization, Iwate Medical University, Iwate, Japan, [g]Center for Medical Genetics, Keio University School of Medicine, Tokyo, Japan, [h]Division of Regenerative Medicine, Institute for Clinical Research, Osaka National Hospital, National Hospital Organization, Osaka, Japan, and [i]Department of Neurosurgery, Osaka National Hospital, National Hospital Organization, Osaka, Japan

Key words: Baraitser-Winter syndrome – *DYRK1A* – *GABRD* – next-generation sequencing

Corresponding author: Nobuhiko Okamoto, Department of Medical Genetics, Osaka Medical Center and Research Institute for Maternal and Child Health, 840, Murodo-cho, Izumi, Osaka 594-1101, Japan.
Tel.: +81 725 56 1220;
fax: +81 725 56 5682;
e-mail: okamoto@osaka.email.ne.jp

Received 26 April 2014, revised and accepted for publication 19 August 2014

Despite many recent studies focusing on discovering the genetic basis of neurodevelopmental diseases, it is still largely unknown. We developed a next-generation sequencing (NGS) based mutation screening strategy. We screened 284 genes known or predicted to be associated with neurodevelopmental disorders with microcephaly/macrocephaly, central nervous system (CNS) anomalies and intellectual disability (ID).

Materials and methods

We studied 40 patients with neurodevelopmental disorders. They were negative for conventional cytogenetic studies and microarray analysis. With the approval of our institutional ethics committee, the patients were analyzed using this targeted sequencing. The genomic DNA of each patient was extracted from peripheral blood using extraction kit. Detail of the cell sample preparation was described in Supporting information.

Target gene sequencing

Three microgram of each sample DNA was sheared to 150–200 bp using the Covaris DNA Shearing System (Wobum, MA, USA). To capture the target exonic DNA, we used the SureSelectXT Custom capture library (Agilent, Santa Clara, CA) for 1.6 Mb of exons of neuronal gene capture. The sequence library was constructed with the SureSelect XT Target Enrichment System for Illumina Paired-End Sequencing Library kit (Agilent) according to the manufacturer's instructions. We performed DNA sequencing of either 76- or 101-bp paired-end reads using the Illumina Genome Analyzer IIx (Illumina, San Diego, CA) and HiSeq 2000 sequencer (Illumina, San Diego, CA).

Single nucleotide variation (SNV) calling

NGS reads were aligned to the Human reference genome (GRCh37/hg19). We then excluded polymerase chain reaction (PCR) duplicates, and extracted reads uniquely mapped to the reference genome that were properly paired within the insert size within mean ± 2 standard deviation (SD) of the mean. Base calling was performed in on-target regions, those regions within 100 bp upstream and downstream of the exon capture probes. SNV and insertion and deletion (indel) calling were performed using SAM TOOLS and GATK software. We excluded known variants found in database. We then narrowed the candidates to only non-synonymous, nonsense and splice site SNVs and frame shift indels. More details of method for variant calling are described in Supporting information.

NGS base-call quality check

To analyze the quality of our base-calling algorithm, we used genotypes from HapMap database (release #28, obtained from ftp://ftp.ncbi.nlm.nih.gov/hapmap/genotypes/2010-08_phaseII+III/). Sanger sequence validation of SNVs was performed using Applied Biosystems 3730xl DNA Analyzer (Life Technologies, Carlsbad, CA).

Results

To identify the causal mutation for neuronal diseases, we designed custom capture probes for the exons of 284 neuronal genes (Table S1, Supporting information). We performed targeted genes sequencing using these probes and generated 1.7 Gb of sequence on average. The average read depth of the on-target regions was 608. To check the quality of our NGS base calls, we sequenced HapMap-JPT NA18943 using the same method as the other samples, and compared our NGS calls with the released genotype of the HapMap consortium. The genotypes for 3129 locations were comparable between the two data sets. All but 16 of the 3129 genotypes were concordant between our NGS calls and the HapMap data. We validated these mismatched 16 positions using Sanger sequencing and all 16 were consistent with our NGS calls (Tables S2 and S3). On the basis of this, we estimate the false positive and false negative rate of our SNV calling to be $<0.032\%$ ($<1/3129$).

Clinical reports

In all patients, developmental quotient (DQ) was measured using the Kyoto Scale of Psychological Development test.

Patient 1 with *ACTB* mutation

The 3-year-old female was born at 37 weeks of gestation by normal delivery. Her developmental milestones were markedly delayed. She sat unsupported at 18 months of age. Recently, she walked with support. She spoke several meaningful words. Her DQ was 39 at 2 years of age. Physical examination identified dysmorphic features, including a flat face, arched eyebrows, narrow palpebral fissures, low-set posteriorly rotated ears and a thin upper lip. Ophthalmological investigation revealed no colobomata. Her height was 86.3 cm (−0.8 SD), and weight was 12.3 kg (mean). Her head circumference was 50 cm (+1.2 SD) at 2 years and 6 months of age. Neuroradiological investigations revealed enlarged lateral ventricles, decreased white matter volume and pachygyria dominant in the frontal lobe (Fig. 1a,b).

A novel missense was identified in *ACTB*, c.733G>A, p.G245S. She was therefore diagnosed with Baraitser-Winter syndrome (BRWS) (1).

Patient 2 with *DYRK1A* mutation

The 7-year-old female patient was born at 39 weeks of gestation by induced delivery. Her developmental milestones were severely retarded. She could not walk independently. She had no communicative language. In addition, her visual acuity was disturbed by severe amblyopia. She could see and reach objects within 30 cm. She exhibited self-injurious behavior, temper tantrums and vocal tics by vibrating her palate. She

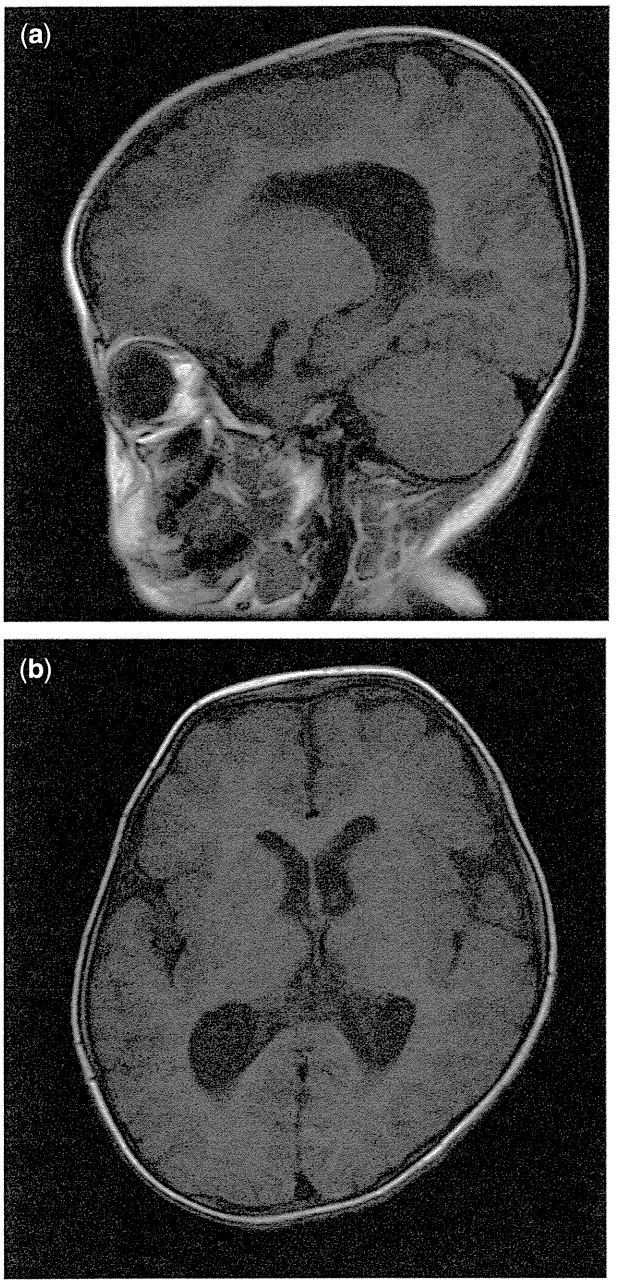

Fig. 1. (**a**, **b**) T1-weighted magnetic resonance image (MR) of patient 1 with *ACTB* mutation shows enlarged lateral ventricles, decreased white matter volume and pachygyria dominant in the frontal lobe.

was diagnosed with autism spectrum disorder (ASD) according to DSM-5. Her DQ was not properly assessed because of visual disturbance.

Physical examination identified dysmorphic features, including frontal bossing, hypertelorism, nystagmus, epicanthal folds, a flat nasal bridge, bilateral low-set ears, down-slanting palpebral fissures, a short philtrum, a high arched palate, downturned mouth and micrognathia. Her weight was 14.6 kg (−2.2 SD), height was 103.5 cm (−3.1 SD) and head circumference was 52 cm (+0.6 SD). She showed relative macrocephaly.

Brain computerized tomography (CT) and magnetic resonance imaging (MRI) were normal. Retinal abnormalities and optic nerve hypoplasia were not identified by fundoscopic investigations. Electroencephalography (EEG) showed no epileptic discharges. She had an early termination codon in exon 11 of the *DYRK1A* gene (c.C1699T: p.Q567*).

Patient 3 with *GABRD* mutation

The 12-year-old female was born at 41 weeks of gestation by induced delivery. Her development was severely retarded with generalized muscular hypotonia. She sat alone at 4 years of age. She cannot walk independently. She spoke no meaningful words. Her DQ was 12 at 9 years of age. She showed stereotyped behavior including hand gripping and bruxism. Purposeful hand skills were not obtained. She was diagnosed with Rett syndrome. EEG revealed bilateral occipital dominant high voltage slow spike and wave complex. Her height was 137 cm (−3.4 SD), weight was 35 kg (−2.1 SD) and head circumference was 51 cm (−1.8 SD). Brain CT and MRI were normal.

She had 2 bp insertion–deletion corresponding to two amino acids in *GABRD* gene (c.G498A:p.M166I and, c.G499A: p.D167N) (Fig. 2). This mutation was *de novo*.

Patient 4 with *PTPN11* mutation

The 4-year-old male was born at 40 weeks of gestation by normal delivery. Profound sensorineural hearing loss was confirmed. He was able to control his head at 4 months, roll over at 6 months of age. He could sit without support at 14 months of age. He started to walk without support at 3 years of age. His height was 90.7 cm (−1.8 SD), weight was 14.3 kg (−0.4 SD) and head circumference was 48.3 cm (−1.1 SD). Brain MRI at 4 years of age showed agenesis of corpus callosum (ACC) (Fig. 3). His DQ was 40. His dysmorphic features including hypertelorism, epicanthal folds, flat nasal bridge, low set ears, growth failure and ACC suggested the diagnosis of Mowat-Wilson syndrome. However, molecular analysis of *ZEB2* mutation was negative. Target gene sequencing revealed a heterozygous mutation in the *PTPN11* gene (c.A188G, p.Y63C). This mutation has been repeatedly reported in Noonan syndrome (NS) (2). We reevaluated his clinical features and concluded that the diagnosis of NS is appropriate. This is the first association of ACC and NS with *PTPN11* mutation.

Other patients

Three patients with cerebellar anomalies were diagnosed with mental retardation and microcephaly with pontine and cerebellar hypoplasia (MICPCH) due to *CASK* mutations. Another patient was homozygous for *AHI1* mutation. The diagnosis of Joubert syndrome was confirmed. They showed typical findings.

Discussion

ACTB mutation in patient 1 was predicted to be pathogenic in *in silico* analysis. BRWS is a rare

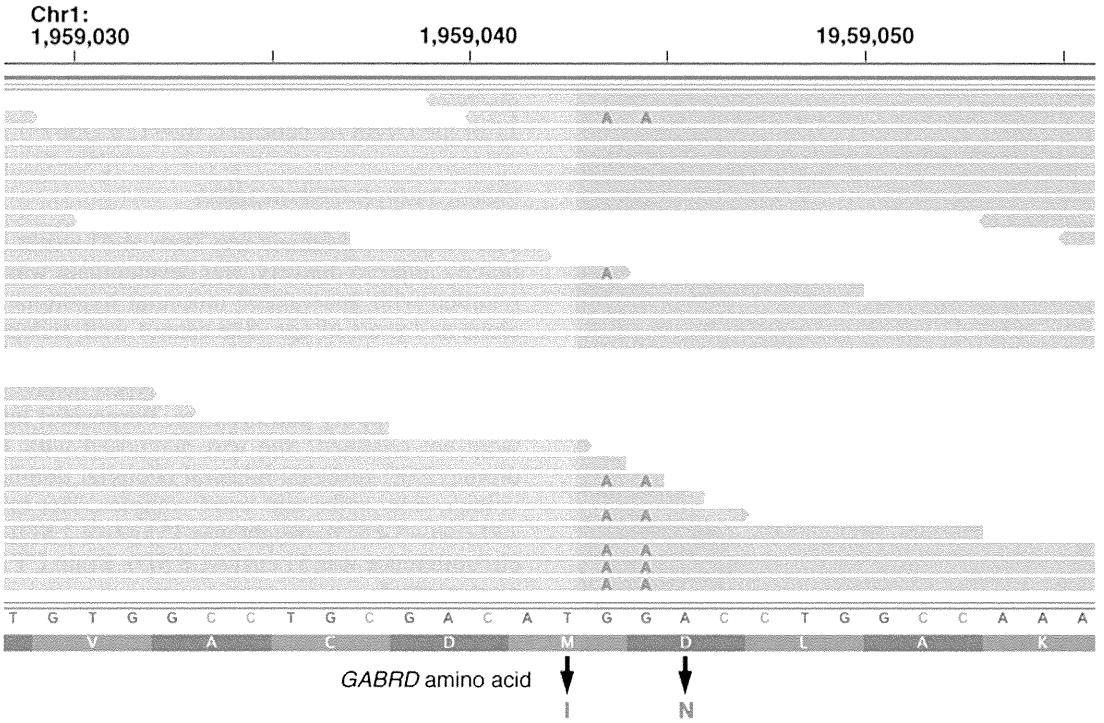

Fig. 2. Patient 3 had 2 bp insertion–deletion corresponding to two amino acids in *GABRD* gene (NM_000815: exon5: c.G498A: p.M166I and NM_000815: exon5: c.G499A: p.D167N).

Fig. 3. Brain magnetic resonance imaging (MRI) of patient 4 with *PTPN11* mutation showed agenesis of corpus callosum

MCA/ID syndrome characterized by dysmorphic features, including ptosis, colobomata and neuronal migration anomalies (1). Rivière et al. (3) reported that mutations in *ACTB* and *ACTG1* cause BRWS. Clinical variability of BRWS is often discussed. Di Donato et al. (4) reported three patients with Fryns-Aftimos syndrome (FAS) who had a mutation in the *ACTB* gene. They suggested that mutations in *ACTB* cause a distinctly more severe phenotype than *ACTG1* mutations. They concluded that FAS is an early and severe manifestation of BRWS. Patient 1 did not show the typical features of BRWS. Her dysmorphic features were mild, and her head circumference was over average size. Recently, Verloes et al. (5) delineated the spectrum in 42 patients with BRWS. They reported that facial dysmorphism varies from mild to severe and evolves considerably over times. They suggested the designation of Baraitser-Winter cerebrofrontofacial syndrome.

Patient 2 had had severe ID, motor disturbance, autistic behavior and visual problems. She had truncating mutation of *DYRK1A*. She lacked microcephaly, which was previously assumed to be a constant feature of *DYRK1A* loss of function. *DYRK1A* is a protein kinase that belongs to the highly conserved dual-specificity tyrosine phosphorylation-regulated kinase (DYRK) family. *DYRK1A* is a highly conserved gene located in the Down syndrome critical region at 21q22. *DYRK1A* is involved in brain growth through neuronal proliferation and neurogenesis. *DYRK1A* overexpression has been implicated in ID and microcephaly in Down syndrome.

Haploinsufficiency of *DYRK1A* is associated with ID, epilepsy and microcephaly (6). So far, mutation analysis of *DYRK1A* has been carried out in patients with ID and microcephaly (7, 8). Courset et al. (9) studied the *DYRK1A* gene in a cohort of 105 patients with ID and Angelman syndrome-like symptoms, and they identified a *de novo* frameshift mutation in a patient with growth retardation, ID, and seizures. O'Roak et al. (10)

captured and sequenced 44 candidate genes in 2446 ASD probands. They discovered 27 *de novo* events in 16 genes including *DYRK1A*. The three patients with a *DYRK1A* mutation showed microcephaly.

We suppose that the clinical spectrum of *DYRK1A* mutations may have more variability. Microcephaly may not be a constant feature in the patients with *DYRK1A* mutations. Another novel finding in patient 2 was severe amblyopia. *Dyrk1A* (+/−) mice showed thin retina (11). We recommend ophthalmologic investigation for patients with *DYRK1A* mutations.

Patient 3 had a 2 bp insertion–deletion corresponding to two amino acids in *GABRD* gene. This is the first report of a *GABRD* mutation associated with Rett syndrome like features. *GABRD* encodes a subunit of the ligand-gated chloride channel for gamma-aminobutyric acid (GABA), the major inhibitory neurotransmitter (12). The majority of GABAA receptors contain two α-subunits, two β-subunits, and a γ- or δ-subunit. Mutations in inhibitory GABAA receptor subunit genes (*GABRA1*, *GABRB3*, *GABRG2* and *GABRD*) have been associated with genetic epilepsy syndromes including childhood absence epilepsy (CAE), juvenile myoclonic epilepsy (JME), pure febrile seizures (FS), generalized epilepsy with febrile seizures plus (GEFS+), and Dravet syndrome (or severe myoclonic epilepsy in infancy).

There have been some reports on the association of generalized epilepsies and *GABRD* mutations. *GABRD* gene is assigned to chromosome 1p36 (13). Patients with the 1p36 deletion syndrome often have epileptic seizures (14). Windpassinger et al. (12) found that *GABRD* is expressed most abundantly in the brain. They suggested that the *GABRD* is a good candidate for the neurodevelopmental and neuropsychiatric anomalies seen in the 1p36 deletion syndrome.

Patient 3 has been diagnosed with Rett syndrome. Heterozygous disruption of *GABRB3* produces increased epileptiform EEG activity and elevated seizure susceptibility in Angelman syndrome (15). We assume that mutant *GABRD* is likely to cause increased neuronal excitability in our patient. Further investigation is necessary to clarify mutations in Rett syndrome-like patients without known genetic causes.

Patient 4 was diagnosed with NS, the most common RASopathy characterized by short stature, distinct facial features, congenital heart defect, and ID of various degrees. Patient 4 showed ACC. So far association of NS and ACC is not known. Hypoplasia of corpus callosum is occasionally reported in cardio-facio-cutaneous syndrome, another RASopathy. We consider ACC to be an unusual manifestation of RASopathy.

Our NGS-based mutation screening strategy showed a certain success in the diagnosis of patients with neurodevelopmental disorders when conventional clinical genetic testing has proven negative. Presented patients showed unique or unexpected manifestations. We are planning whole-exome sequencing for the remaining unexplained patients.

Supporting Information

Additional supporting information may be found in the online version of this article at the publisher's web-site.

Acknowledgements

This study was supported by a grant from the Research on Applying Health Technology from the Ministry of Health, Labor and Welfare of Japan. We thank the patients and their families for participating in this work. We thank Mr K. A. Boroevich for English proofreading.

References

1. Baraitser M, Winter RM. Iris coloboma, ptosis, hypertelorism, and mental retardation: a new syndrome. J Med Genet 1988: 25: 41–43.
2. Tartaglia M, Mehler EL, Goldberg R et al. Mutations in PTPN11, encoding the protein tyrosine phosphatase SHP-2, cause Noonan syndrome. Nat Genet 2001: 29: 465–468.
3. Rivière JB, van Bon BW, Hoischen A et al. De novo mutations in the actin genes ACTB and ACTG1 cause Baraitser-Winter syndrome. Nat Genet 2012: 44: 440–444.
4. Di Donato N, Rump A, Koenig R et al. Severe forms of Baraitser-Winter syndrome are caused by ACTB mutations rather than ACTG1 mutations. Eur J Hum Genet 2014: 22: 179–183.
5. Verloes A, Di Donato N, Masliah-Planchon J et al. Baraitser-Winter cerebrofrontofacial syndrome: delineation of the spectrum in 42 cases. Eur J Hum Genet 2014 Jul 23. doi: 10.1038/ejhg.2014.95. [Epub ahead of print]
6. Moller RS, Kubart S, Hoeltzenbein M et al. Truncation of the Down syndrome candidate gene DYRK1A in two unrelated patients with microcephaly. Am J Hum Genet 2008: 82: 1165–1170.
7. Yamamoto T, Shimojima K, Nishizawa T et al. Clinical manifestations of the deletion of Down syndrome critical region including DYRK1A and KCNJ6. Am J Med Genet A 2010: 155A: 113–119.
8. Valetto A, Orsini A, Bertini V et al. Molecular cytogenetic characterization of an interstitial deletion of chromosome 21 (21q22.13q22.3) in a patient with dysmorphic features, intellectual disability and severe generalized epilepsy. Eur J Med Genet 2012: 55: 362–366.
9. Courcet JB, Faivre L, Malzac P et al. The DYRK1A gene is a cause of syndromic intellectual disability with severe microcephaly and epilepsy. J Med Genet 2012: 49: 731–736.
10. O'Roak BJ, Vives L, Fu W, Egertson JD et al. Multiplex targeted sequencing identifies recurrently mutated genes in autism spectrum disorders. Science 2012: 338: 1619–1622.
11. Laguna A, Barallobre MJ, Marchena MÁ et al. Triplication of DYRK1A causes retinal structural and functional alterations in Down syndrome. Hum Mol Genet 2013: 22: 2775–2784.
12. Windpassinger C, Kroisel PM, Wagner K et al. The human gamma-aminobutyric acid A receptor delta (GABRD) gene: molecular characterisation and tissue-specific expression. Gene 2002: 292: 25–31.
13. Emberger W, Windpassinger C, Petek E et al. Assignment of the human GABAA receptor delta-subunit gene (GABRD) to chromosome band 1p36.3 distal to marker NIB1364 by radiation hybrid mapping. Cytogenet Cell Genet 2000: 89: 281–282.
14. Rosenfeld JA, Crolla JA, Tomkins S et al. Refinement of causative genes in monosomy 1p36 through clinical and molecular cytogenetic characterization of small interstitial deletions. Am J Med Genet A 2010: 152A: 1951–1959.
15. DeLorey TM, Olsen RW. GABA and epileptogenesis: comparing gabrb3 gene-deficient mice with Angelman syndrome in man. Epilepsy Res 1999: 36: 123–132.

CLINICAL REPORT

AMERICAN JOURNAL OF medical genetics PART A

A Clinical Study of Patients With Pericentromeric Deletion and Duplication Within 16p12.2–p11.2

Nobuhiko Okamoto,[1]* Tatsuya Fujii,[2] Junko Tanaka,[3] Kazumasa Saito,[4] Takeshi Matsui,[4] and Naoki Harada[4]

[1]Department of Medical Genetics, Osaka Medical Center and Research Institute for Maternal and Child Health, Osaka, Japan

[2]Department of Pediatrics, Shiga Medical Center for Children, Moriyama, Shiga, Japan

[3]Tanaka-Kitaumeda Clinic, Osaka, Japan

[4]Department of Molecular Genetic Research, Mitsubishi Chemical Medience Corporation, Tokyo, Japan

Manuscript Received: 16 July 2012; Manuscript Accepted: 8 August 2013

The short arm of chromosome 16 is rich in segmental duplications that result in chromosomal rearrangements through non-allelic homologous recombination. Several syndromes resulting from microdeletions or microduplications in this region have been reported. The chromosome 16p12.2–p11.2 deletion syndrome, 7.1- to 8.7-Mb [OMIM#613604] is characterized by minor facial anomalies, feeding difficulties, a significant delay in speech development, and recurrent ear infections. Reciprocal duplications of 16p12.2–p11.2 have been reported in some patients with autism. We identified a patient with a 16p12.2–p11.2 deletion and a patient with a 16p12.2–p11.2 duplication using oligonucleotide SNP array. The patient with the deletion showed severe developmental delay without autism. The patient with the deletion shared clinical features with previously reported patients. The patient with the duplication showed mild developmental delay and autism. She had dysmorphic features including a round face, a large mouth, and relative macrocephaly. We reviewed the reports of the two syndromes and compared the clinical manifestations. The 16p12.2–p11.2 duplication syndrome is a new syndrome with autism spectral disorders and dysmorphic features. © 2013 Wiley Periodicals, Inc.

Key words: 16p12.2–p11.2 deletion; 16p12.2–p11.2 duplication; SNP array; chromosomal aberration

How to Cite this Article:
Okamoto N, Fujii T, Tanaka J, Saito K, Matsui T, Harada N. 2013. A clinical study of patients with pericentromeric deletion and duplication within 16p12.2–p11.2.
Am J Med Genet Part A 9999:1–7.

INTRODUCTION

Several recurrent copy number variations are known in the pericentromeric region of chromosome16p. This region is rich in segmental duplications that result in chromosomal rearrangements through non-allelic homologous recombination.

Weiss et al. [2008] identified a novel, recurrent microdeletion, and a reciprocal microduplication at 16p11.2 with susceptibility to autism spectrum disorders (ASD) which appeared among approximately 1% of cases. Kumar et al. [2008] reported more patients. Chromosome 16p11.2 deletion syndrome [MIM#611913] (29.5–30.1 Mb) is observed in about 1% of patients with ASD [Fernandez et al., 2010].

Bochukova et al. [2010] identified five patients with overlapping deletions at 16p11.2 including *SH2B1* which is associated with leptin and insulin signaling. In three of these patients, a 220-kb deletion (28.73–28.95 Mb) was inherited from an obese parent and segregated with severe early-onset obesity without developmental problems. The other two patients showed a de novo 1.7-Mb deletion at 16p11.2 extending through the proximal 593-kb region of 16p11.2. The two patients had mild developmental delay and severe early-onset obesity. Bachmann-Gagescu et al. [2010] identified 31 patients with deletions of the *SH2B1*-containing region and supported the association of developmental delays and obesity.

Girirajan et al. [2010] suggested a 2-hit model in a recurrent 520-kb heterozygous microdeletion of 16p12. Probands with the 16p12.1 microdeletion were more likely to have additional large deletions or duplications, and the clinical features of individuals with the 16p12 deletion and additional CNV were distinct from and/or more severe than those with the 16p12.1 microdeletion only.

Conflict of interest: none.
Grant sponsor: Ministry of Health, Labor and Welfare in Japan.
*Correspondence to:
Dr. Nobuhiko Okamoto, Department of Medical Genetics, Osaka Medical Center, Research Institute for Maternal, Child Health, 840 Murodo-cho, Izumi, Osaka 594-1101, Japan.
E-mail: okamoto@osaka.email.ne.jp
Article first published online in Wiley Online Library (wileyonlinelibrary.com): 00 Month 2013
DOI 10.1002/ajmg.a.36217